

## Orally Bioavailable Antagonists of Inhibitor of Apoptosis Proteins Based on an Azabicyclooctane Scaffold<sup>∞</sup>

Frederick Cohen,<sup>\*,†</sup> Bruno Alicke,<sup>‡</sup> Linda O. Elliott,<sup>#</sup> John A. Flygare,<sup>†</sup> Tatiana Goncharov,<sup>||</sup> Stephen F. Keteltas,<sup>†</sup> Matthew C. Franklin,<sup>||</sup> Stacy Frankovitz,<sup>⊥</sup> Jean-Philippe Stephan,<sup>⊥</sup> Vickie Tsui,<sup>†</sup> Domagoj Vucic,<sup>||</sup> Harvey Wong,<sup>§</sup> and Wayne J. Fairbrother<sup>||</sup>

Departments of Discovery Chemistry, Translational Oncology, Biochemical Pharmacology, Protein Engineering, Assay and Automation Technology, and Drug Metabolism and Pharmacokinetics, Genentech, Inc., 1 DNA Way, South San Francisco, California 94080

Received November 17, 2008

A series of IAP antagonists based on an azabicyclooctane scaffold was designed and synthesized. The most potent of these compounds, **14b**, binds to the XIAP BIR3 domain, the BIR domain of ML-IAP, and the BIR3 domain of c-IAP1 with  $K_i$  values of 140, 38, and 33 nM, respectively. These compounds promote degradation of c-IAP1, activate caspases, and lead to decreased viability of breast cancer cells without affecting normal mammary epithelial cells. Finally, compound **14b** inhibits tumor growth when dosed orally in a breast cancer xenograft model.

### Introduction

Programmed cell death, or apoptosis, is a crucial mechanism for maintaining homeostasis and removal of damaged or malignant cells. This pathway is tightly controlled by a number of positive and negative regulatory elements. The inhibitor of apoptosis (IAP<sup>a</sup>) proteins negatively regulate this process through a variety of mechanisms including direct inhibition of effector caspase enzymes or modulation of TNF receptor-mediated signaling pathways.<sup>1–6</sup> Members of this family are up-regulated in various cancers and promote resistance to chemotherapy. Thus, inhibition of these proteins may be a new therapeutic mechanism for treating cancer.<sup>7,8</sup>

Each of the IAP proteins contains at least one BIR domain, some of which bind to the N-termini of their targets through interactions with a shallow cleft. Although the peptide-binding pocket of the BIR domains is shallow, several groups have reported peptidomimetics<sup>9–12</sup> or other small molecules<sup>13–16</sup> that bind to this pocket with high affinity, disrupt IAP-caspase or IAP-SMAC binding, and show in vivo efficacy in a mouse xenograft model of cancer.<sup>17,18</sup>

In this communication we report our initial efforts toward developing a molecule with reduced peptide character that would possess the appropriate potency, permeability, and pharmacokinetic properties to be a useful therapeutic agent. To generate ideas for small molecule scaffolds that could potentially displace

parts of the peptide, the software program CAVEAT was utilized.<sup>19</sup> This program takes as input the structure of a peptide or small molecule bound in the target receptor site. Selected bond vectors are searched against prebuilt databases of three-dimensional compounds to find ring systems that could connect to and maintain the vectors in their input spatial arrangement.

We used the 2.3 Å resolution crystal structure of peptide Ala-Val-Pro-2,2-diphenethylamine (**1**) bound to the ML-IAP BIR domain as the input structure (Figure 1A).<sup>20</sup> One vector was defined from the proline nitrogen atom to the valine carbonyl carbon atom, while a second vector was defined from the proline carbonyl carbon atom to the diphenethylamine nitrogen (Figure 2A). CAVEAT databases of minimized compounds from commercially available small molecules were constructed and searched. Ring systems that overlapped with atoms of the ML-IAP BIR domain were not considered in subsequent analyses.

The conformations and qualitative geometric fit of all unique hits were examined visually. In particular, some fused-ring motifs (Figure 2B) looked especially promising from a geometric perspective. However, upon further inspection, these were deemed either synthetically infeasible within our desired time frame or chemically unstable. These bicyclic motifs provided the inspiration to manually search the literature for similar bicyclic templates that would be more synthetically accessible; from this search emerged an azabicyclooctane (Figure 2C). A further conceptual jump was to realize that use of this scaffold would also require reversing the direction of the P3–P4 amide bond for both synthetic accessibility and geometric fit.

When the azabicyclooctane scaffold was computationally inserted into the rest of the peptide, using a reversed amide to link the diphenyl group to the scaffold (Figure 2D), it was found to fit well within the peptide binding site. Using Glide, a minimized conformation of this molecule was docked to the ML-IAP BIR domain peptide-binding site.<sup>21</sup> The conformations that emerged were similar to the conformations of **1** both in the crystal structure and in the docked model (Figure 1B). The docking score of the azabicyclooctane compound (–9.5) is comparable to that of **1** (–9.3). The main difference between the crystal structure and docked models relates to which of the prochiral phenyl groups is buried in the P4 pocket. In the crystal structure of **1**, the *pro-S* phenyl ring of the 2,2-diphenylethylamine moiety packs into the hydrophobic P4 pocket where it

<sup>∞</sup> Coordinates and structure factors have been deposited in the RCSB Protein Data Bank. Access codes are as follows: **1**, 3F7G; **14a**, 3F7H; **14b**, 3F7I.

\* To whom correspondences should be addressed. Phone: 650-225-2976. Fax: 650-467-8922. E-mail: fcohen@gene.com.

<sup>†</sup> Department of Discovery Chemistry.

<sup>‡</sup> Department of Translational Oncology.

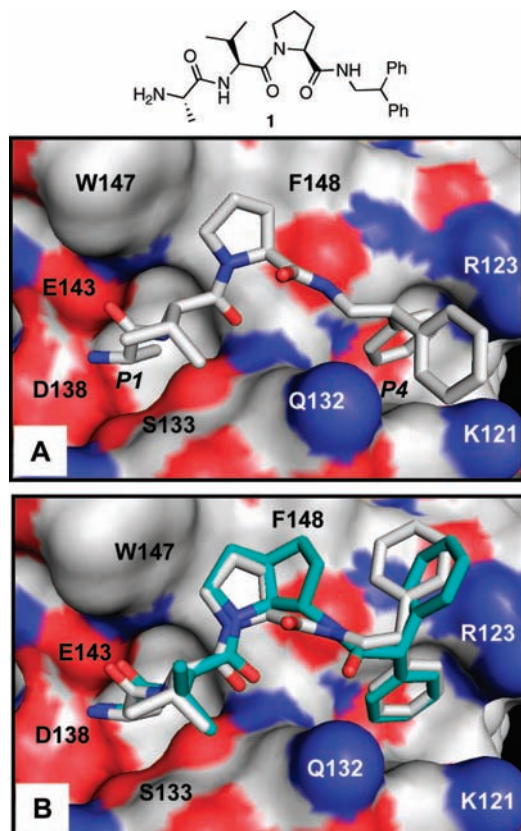
<sup>#</sup> Department of Biochemical Pharmacology.

<sup>||</sup> Department of Protein Engineering.

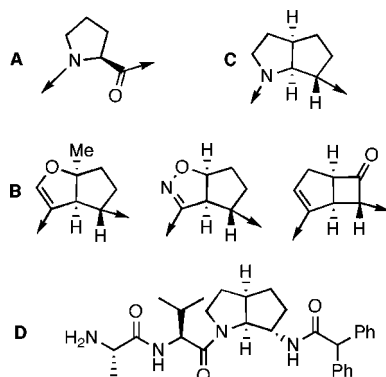
<sup>⊥</sup> Department of Assay and Automation Technology.

<sup>§</sup> Department of Drug Metabolism and Pharmacokinetics.

<sup>a</sup> Abbreviations: IAP, inhibitor of apoptosis; XIAP, X-chromosome-linked inhibitor of apoptosis; BIR, baculoviral inhibitor of apoptosis repeat; ML-IAP, melanoma inhibitor of apoptosis; SMAC, second mitochondrial activator of caspase; Teoc, (trimethylsilyl)ethyl carbamate; TFA, trifluoroacetic acid; TMS, trimethylsilyl; EDC, *N*-(3-dimethylaminopropyl)-*N'*-ethylcarbodiimide hydrochloride; HATU, 2-(7-aza-1*H*-benzotriazole-1-yl)-1,1,3,3-tetramethyluroniumhexafluorophosphate; TASF, tris(dimethylamino)sulfonium difluorotrimethylsilicate; HMEC, human mammary epithelial cells.



**Figure 1.** (A) Crystal structure of the ML-IAP BIR domain in complex with **1**. The key P1 and P4 binding pockets are labeled. (B) Overlay of the highest-scoring docked Ala-Val-Pro-2,2-diphenethylamine conformation (gray) and the highest-scoring docked azabicyclooctane compound (Figure 2D) (cyan) in the ML-IAP peptide-binding site.



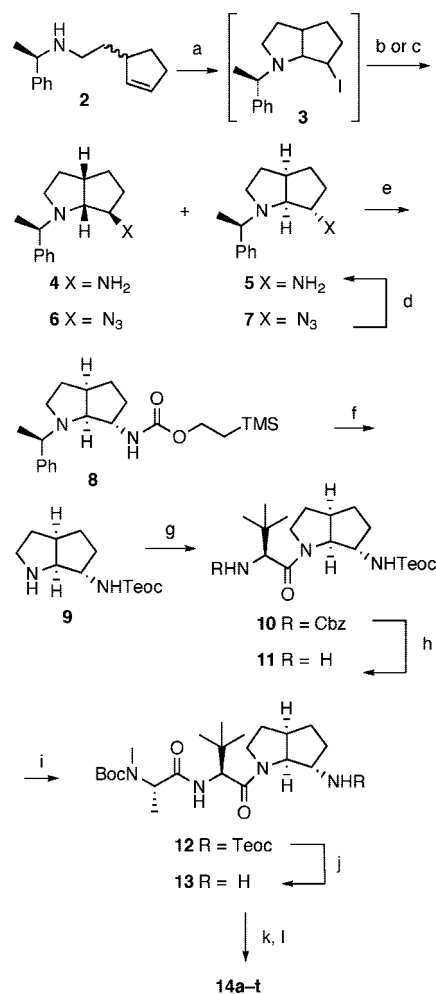
**Figure 2.** Evolution of azabicyclooctane proline mimetic: (A) input vectors for CAVEAT search; (B) bicyclic hits from CAVEAT search; (C) azabicyclooctane inspired by search hits; (D) elaborated construct used to compare scaffold design to **1**.

makes extensive contacts with protein residues Thr116, Lys121-Arg123, and Gly130-Gln132 (Figure 1A). The second (*pro-R*) phenyl ring of the 2,2-diphenylethylamine moiety packs more on the surface of the protein with one edge making contact with the hydrophobic portion of the side chain of Lys121. By contrast, both models predicted that the *pro-R* phenyl group would insert into the P4 pocket and the *pro-S* phenyl group would be more exposed (Figure 1B).

## Synthesis

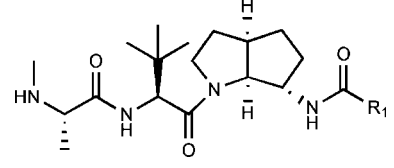
The synthesis of this scaffold is based on the work of Corey<sup>22</sup> and Kawabata.<sup>23</sup> We began with amine **2**, which when treated

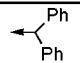
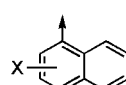
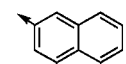
## Scheme 1. Synthesis of Amide Analogues **14a-t**



<sup>a</sup> Reagents and conditions: (a)  $I_2$ ,  $CH_2Cl_2$ . (b) **4** and **5**:  $NH_4OH$ , THF, HPLC separation, 29%, two steps. (c) **6** and **7**:  $NaN_3$ , acetone, water; SiO<sub>2</sub> separation 35%, two steps; (d) 10% Pd·C, 1 atm of  $H_2$ , EtOAc, 94%; (e)  $TMSCH_2CH_2OC(O)OC_6H_4NO_2$ ,  $NaHCO_3$ ,  $CH_2Cl_2$  55%; (f)  $H_2$ , 20% Pd(OH)<sub>2</sub>·C, MeOH, quant; (g) Cbz-*t*-Leu-OH, HATU, DIPEA, DMF; (h)  $H_2$ , 20% Pd(OH)<sub>2</sub>·C, MeOH, 72% two steps; (i) Boc-*N*-Me-Ala-OH, EDC, DMAP, MeCN; (j) TASF, MeCN, 50 °C, 88–94%, two steps; (k)  $R_1COCl$  or  $R_1CO_2H$ , EDC, DMAP, MeCN; (l) TFA,  $CH_2Cl_2$ , HPLC purification, 16–79% two steps.

with  $I_2$  in  $CH_2Cl_2$  provided bicyclic amino iodide **3** (Scheme 1). Subjection of this crude mixture to  $NH_4OH$  and THF led to displacement of the iodide by ammonia, with retention of configuration, providing diastereomeric diamines **4** and **5**. These compounds were separated by HPLC on a C<sub>18</sub> column, eluting with 0–10% MeCN/H<sub>2</sub>O, 0.1% trifluoroacetic acid (TFA). The desired diastereomer **5** elutes first under these conditions. Assignment of the stereochemistry of **4** and **5** was made initially by carrying both isomers forward to IAP antagonists and comparing potency in the fluorescence polarization assay. Our assignment was subsequently verified by X-ray analysis of a cocrystal of an antagonist with an IAP BIR domain (vide infra). While acceptable for making exploratory quantities of these compounds, the requirement for separating diastereomers by HPLC limited our ability to make larger amounts of material and led us to investigate another nitrogen source. Thus, treatment of iodide **3** with sodium azide in a mixture of acetone–water cleanly led to a mixture of azides **6** and **7**, which were separable on silica gel, greatly improving throughput. Hydrogenation under mild conditions provided the primary amine **5**, with no trace of benzyl deprotection.

**Table 1.** Structure and Potency of IAP Selected Antagonists<sup>a</sup>


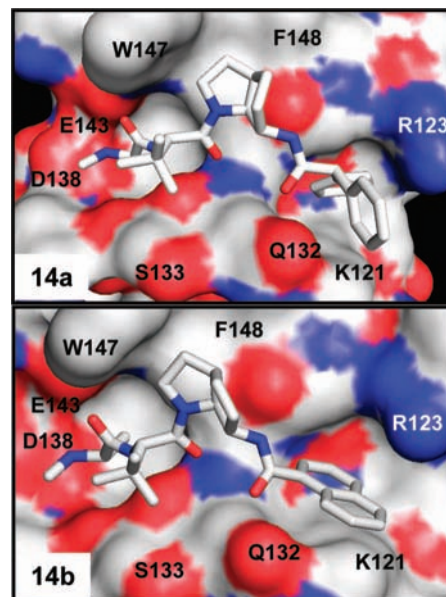
Compound	R <sub>1</sub>	K <sub>i</sub> (μM) <sup>b</sup>	
		XIAP-BIR3	MLXBIR3SG
<b>14a</b>		0.57	0.082
<b>14b</b>		X = H	0.140
<b>14c</b>	X = 4-F	0.210	0.038
<b>14d</b>	X = 4-Me	0.190	0.063
<b>14e</b>	X = 2-OMe	0.11	0.11
<b>14f</b>		1.20	0.091

<sup>a</sup> K<sub>i</sub> determined as described in ref 10. <sup>b</sup> Average of two measurements.

After experimenting with several protecting group schemes, we arrived at (trimethylsilyl)ethyl carbamate (Teoc) as the optimal group for the primary amine. Thus, the primary amine of **5** was acylated with Teoc-*p*-nitrophenyl carbonate under biphasic conditions, and the benzyl group was removed by hydrogenolysis with 20% Pd(OH)<sub>2</sub>·C, to provide amine **9** in 46% yield for the two steps. We chose to fix the P1 and P2 amino acids as *N*-Me-Ala and *tert*-Leu, respectively, for this study, as SAR in the peptide series demonstrated that these changes retained potency and afforded increased hydrolytic stability (data not shown). Thus, coupling of Cbz-protected *tert*-Leu was accomplished with *N*-(3-dimethylaminopropyl)-*N'*-ethylcarbodiimide hydrochloride (EDC) and the Cbz group removed with H<sub>2</sub> and 20% Pd(OH)<sub>2</sub>·C to afford amine **11** in 72% yield over two steps. The P1 amino acid was coupled in Boc-protected form with EDC. Finally, the Teoc group was removed with tris(dimethylamino)sulfonium difluorotrimethylsilicate (TASF) in warm MeCN.<sup>24</sup> This route was readily amenable to preparation of half-gram quantities of common intermediate **13**.

With common intermediate **13** in hand, we sought to explore the SAR of the P4 position. Carboxylic acid derivatives were selected by a combination of computational virtual reagent selection and medicinal chemistry principles. These were coupled through either the acid chloride or EDC dehydration. The Boc group was removed with TFA, and the final product was purified by HPLC. The structures of the most potent antagonists **14a–f**, made via this route, are shown in Table 1. A complete list of the antagonists synthesized is in the Supporting Information.

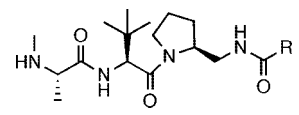
The K<sub>i</sub> values binding to the BIR3 domain of XIAP and the single BIR domain of ML-IAP were determined using a fluorescence polarization competition assay.<sup>10</sup> The results are

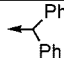
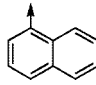
**Figure 3.** Crystal structures of **14a** and **14b** in complex with MLXBIR3SG at 1.8 and 1.9 Å resolution, respectively.

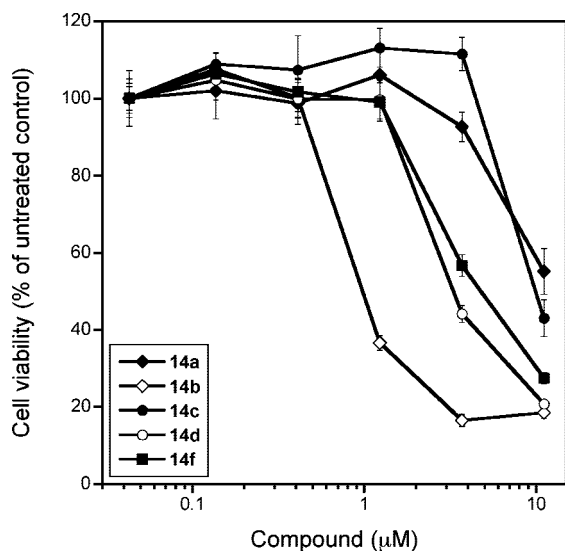
summarized in Table 1. The potency of diphenylacetamide derivative **14a** was within 2-fold of the potency of the peptide lead **1** (K<sub>i</sub> = 43 nM for MLXBIR3SG, a chimeric BIR domain that preserves the native ML-IAP peptide-binding site,<sup>20</sup> and K<sub>i</sub> = 345 nM for XIAP BIR3). Most of the other moieties chosen for the P4 position lost potency relative to the starting peptide. However, a series of 1-naphthyl derivatives **14b–e** retained or increased affinity for both MLXBIR3SG and XIAP BIR3. The 2-naphthyl isomer **14f** lost affinity for XIAP BIR3 and retained affinity for MLXBIR3SG, making it the most selective compound in the series. This series also shows that polar substituents are not tolerated in the P4 pocket.

To gain a more detailed understanding of the interactions between the azabicyclooctane-containing IAP antagonists and the BIR domain of ML-IAP, the crystal structures of complexes between MLXBIR3SG and compounds **14a** and **14b** were determined to resolutions of 1.8 and 1.9 Å, respectively (Figure 3). X-ray data collection and refinement statistics are listed in Supporting Information Table 1. Key contacts observed in the structure of **1** in complex with the ML-IAP BIR domain (Figure 1A) are conserved in the complexes with **14a** and **14b**. In particular, hydrogen bonds with the main chain of Gln132 and the side chain carboxylate of Asp138 are maintained. In the case of **14a**, the phenyl rings of the diphenylacetamide moiety are positioned very similarly to the phenyl rings of the 2,2-diphenylethylamine moiety of **1**. The 1-naphthyl group of **14b** also makes extensive contacts with the hydrophobic P4 pocket of the protein, although in order to make these contacts, the conformations of the azabicyclooctane and the intervening amide group differ slightly from that observed for **14a**.

The azabicyclooctane scaffold both reverses the direction of the P3–P4 amide bond and adds extra conformational constraint relative to **1**. We sought to dissect these two effects through the synthesis of control molecules. Thus, the two peptides **15a** and **15b** (Table 2) were synthesized using routine peptide chemistry from *S*-2-(aminomethyl)-1-*tert*-butoxycarbonylpyrrolidine. These compounds lack the constraint of the bicyclic scaffold and yet retain the reversal of the P3–P4 amide bond. Compound **15a** lost approximately 3- to 5-fold in binding affinity relative to **14a**, while **15b** lost approximately 10- to 15-fold in binding affinity relative to **14b**. These data show that

**Table 2.** Potency of Monocyclic Controls<sup>a</sup>


Compound	R <sub>1</sub>	K <sub>i</sub> (μM) <sup>b</sup>	
		XIAP-BIR3	MLXBIR3SG
<b>15a</b>		3.0	0.29
<b>15b</b>		1.60	0.78

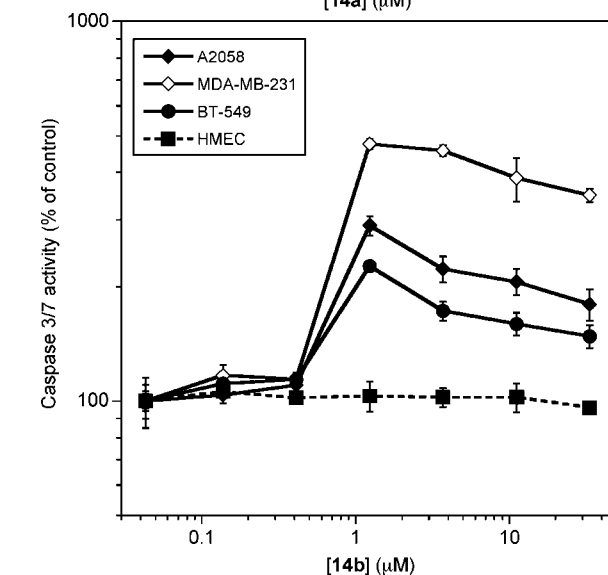
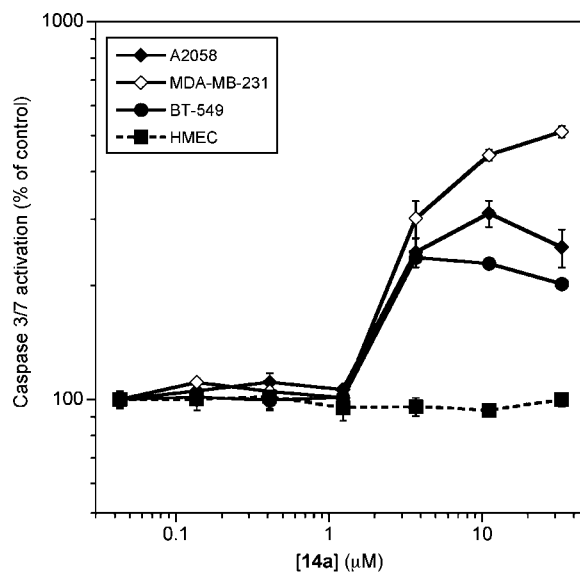
<sup>a</sup> K<sub>i</sub> determined as described in ref 10. <sup>b</sup> Average of two measurements.**Figure 4.** Cell-killing in response to 3 day treatment with IAP antagonists in MDA-MB-231 cells.**Table 3.** EC<sub>50</sub> Values for Selected Compounds in 3-Day Cell Viability Assay (Values in μM, Average of Three Determinations)

compd	EC <sub>50</sub> (μM)	
	MDA-MB-231	HMEC
<b>14a</b>	9.64 ± 1.00	>10
<b>14b</b>	0.98 ± 0.14	>10
<b>14c</b>	10.2 ± 0.30	>10
<b>14d</b>	3.12 ± 0.69	>10
<b>14f</b>	3.29 ± 0.11	>10

the extra ring provided by the scaffold has a significant contribution to the potency of these antagonists.

A selection of the more potent IAP antagonists were tested in 3-day cell-viability assays (Figure 4, Table 3). These compounds led to a decrease in cell viability in the MDA-MB-231 breast cancer cell line. This is in contrast to starting peptide **1**, which does not induce cell death in a 3-day viability assay. These compounds did not cause cell death in normal human mammary epithelial cells (HMEC).

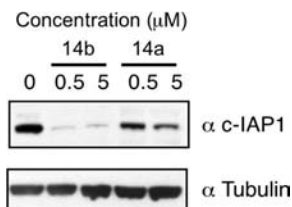
To assess the mechanism of cell killing, these compounds were tested for activation of the effector caspases 3 and 7 in the breast cancer cell lines BT-549 and MDA-MB-231. These compounds were found to activate caspases 3 and 7 in a dose dependent manner. The potency in the caspase activation assay

**Figure 5.** Caspase 3/7 activation in response to treatment with **14a** and **14b** for 6 h in various cell lines.**Table 4.** EC<sub>50</sub> for Caspase Activation in Cell Culture

compd	EC <sub>50</sub> (μM)		
	MDA-MB-231	BT-549	HMEC
<b>14a</b>	3.59 ± 0.20	1.81 ± 0.45	>10
<b>14b</b>	0.49 ± 0.01	0.47 ± 0.02	>10
<b>14c</b>	4.45 ± 0.03	4.07 ± 0.11	>10
<b>14d</b>	1.58 ± 0.11	1.45 ± 0.04	>10
<b>14f</b>	1.32 ± 0.04	0.19 ± 0.01	>10

correlates well with the potency in the viability assay. Example data for compounds **14a** and **14b** are shown in Figure 5, and potencies are tabulated in Table 4. Consistent with the viability assays, these compounds did not activate effector caspases in normal human mammary epithelial cells (HMEC).

The effects of the IAP antagonist compounds **14a** and **14b** on the stability of c-IAP1 protein were also examined. Treatment of MDA-MB-231 breast carcinoma cells with **14a** for 1 h had only a minor effect on the levels of c-IAP1, while similar treatment with **14b** led to almost complete loss of c-IAP1 protein (Figure 6) in agreement with reported studies.<sup>2,4</sup> These data correlate with the measured potency of **14a** and **14b** against the c-IAP1 BIR3 domain (**14a** K<sub>i</sub> = 129 nM; **14b** K<sub>i</sub> = 33 nM).



**Figure 6.** Treatment with IAP antagonist compound **14b** leads to degradation of c-IAP1. MDA-MB-231 cells were treated for 1 h with the indicated concentrations of **14b** or **14a**, and cell lysates were probed with the indicated antibodies.

In preparation for efficacy studies, compounds **14a** and **14b** were evaluated for oral exposure in mice. Thus, each was dosed at 25 mg/kg as a solution in 15% aqueous hydroxypropyl- $\beta$ -cyclodextrin with 20 mM succinic acid. Both compounds were found to have significant exposure upon oral dosing. Compound **14a** was found to have a  $C_{\text{max}}$  of 5.0  $\mu\text{M}$ , AUC of 16 h $\cdot\mu\text{M}$ , and  $T_{1/2}$  of 1.5 h, while **14b** was found to have a  $C_{\text{max}}$  of 3.6  $\mu\text{M}$ , AUC of 5.0 h $\cdot\mu\text{M}$ , and  $T_{1/2}$  of 1.3 h.

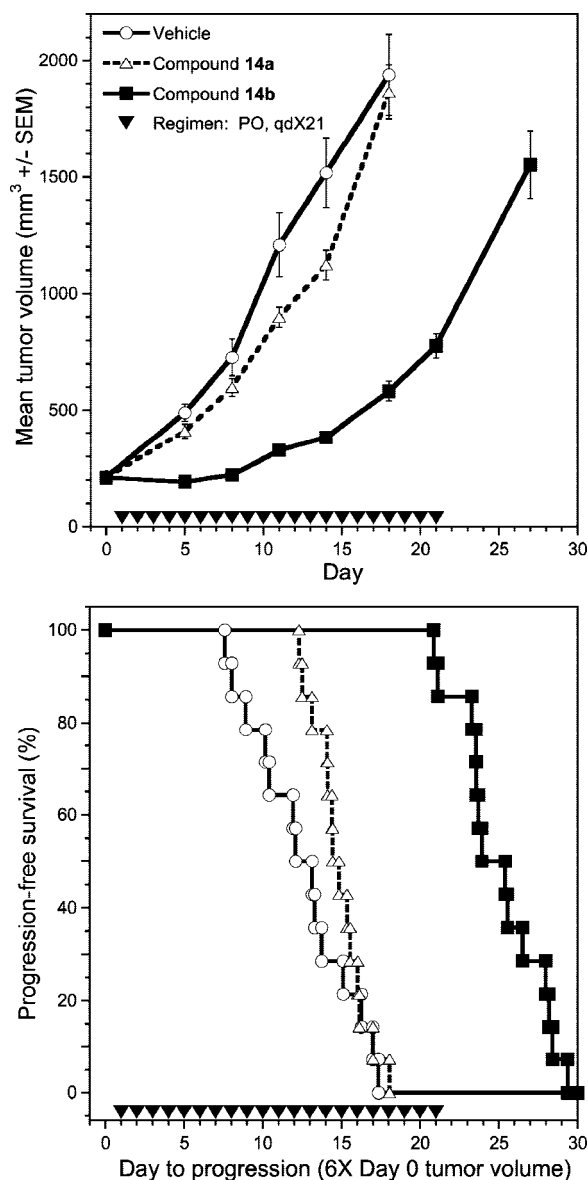
Compounds **14a** and **14b** were further studied in a mouse cancer xenograft model (Figure 7). To that effect, mice bearing tumors ( $n = 14$  per group) derived from the MDA-MD-231 cell line were dosed orally with either vehicle or compounds at 50 (mg/kg)/day. Compound **14b** potently inhibited tumor growth in this model, with a median time to progression (defined as time to 6-fold increase in tumor volume from day 0) of 25 days, versus 14 days for the vehicle control, without affecting body weight. Compound **14a** had little effect on either tumor growth or body weight.

## Conclusion

We have designed and synthesized a novel azabicyclooctane proline mimetic and incorporated it into IAP antagonists. Several of these compounds were more potent than lead peptide **1**, with  $K_i$  values of <50 nM against select IAP BIR domains. X-ray crystallographic analysis confirmed that these compounds bind to the expected binding site on the ML-IAP BIR domain. These compounds induce degradation of c-IAP1 and activate effector caspases in cancer cell lines in preference to normal cell lines. Compounds that potently activated caspases also lead to decreased viability of cancer cell lines without affecting "normal", nontumor cells. This potency in cell culture assay translates to significant potency in a xenograft model of breast cancer where compound **14b** nearly doubles the time to progression when dosed orally. These studies further validate the IAP proteins as promising targets for cancer treatment.

## Experimental Section

All chemicals were purchased from commercial suppliers (Aldrich, VWR) and used as received. Flash chromatography was carried out with RediSep prepacked  $\text{SiO}_2$  cartridges on an ISCO Companion chromatography system. NMR spectra were recorded on a Varian Inova 400 NMR spectrometer and referenced to tetramethylsilane. For all compounds that contain secondary amides the data for the major rotamers are reported. Preparative HPLC was performed on a Polaris  $\text{C}_{18}$  5  $\mu\text{m}$  column (50 mm  $\times$  21 mm). Purity analysis of final compounds was performed by HPLC-MS with a Chromasil  $\text{C}_{18}$  column (4.6 mm  $\times$  50 mm) with a gradient of 0–90% acetonitrile (containing 0.038% TFA) in 0.1% aqueous TFA (over 11 min, flow = 2 mL/min). Low-resolution mass spectra were recorded on a Sciex 15 mass spectrometer in ES+ mode. Purity analysis of final compounds was also performed on a Berger Instruments SFC system operating at 100 bar, 35  $^\circ\text{C}$ , column = Berger diol, 4.6 mm  $\times$  150 mm, with a 6 min gradient of 20–60%



**Figure 7.** Efficacy of compounds **14a** and **14b** compared to vehicle control. Compounds were dosed 50 (mg/kg)/day po,  $n = 14$  per group.

MeOH in  $\text{CO}_2$  flowing at 2.35 mL/min (SFCd method) or a Berger pyridine column, 4.6 mm  $\times$  150 mm, with a 6 min gradient of 5–50% MeOH in  $\text{CO}_2$  flowing at 2.35 mL/min (SFCp). All final compounds were purified to >95% purity. High-resolution mass spectra were obtained at the University of California at Berkeley on a ZAB2-EQ mass spectrometer (Micromass, Manchester, U.K.) equipped with a FAB ion source. The source was operated at 8 kV; the Cs gun was operated at 20 kV.

**(3aS,6S,6aR)-1-((R)-1-Phenylethyl)octahydrocyclopenta[b]pyrrol-6-ylamine (4)** and **(3aR,6S,6aS)-1-((R)-1-Phenylethyl)octahydrocyclopenta[b]pyrrol-6-ylamine (5)**. To a solution of amine **2** (3.13 g, 14.5 mmol) in  $\text{CH}_2\text{Cl}_2$  (60 mL) was added  $\text{I}_2$  (4.43 g, 17.4 mmol) portionwise over 30 min with vigorous stirring. After 2 h, LCMS indicated complete conversion to iodide **3**. The mixture was concentrated under reduced pressure to afford a dark-brown foam.

The residue from above was dissolved in THF (50 mL) and concentrated  $\text{NH}_4\text{OH}$  (50 mL) and stirred at room temperature for 17 h. The THF was removed under reduced pressure and the residue diluted with 1 N NaOH (50 mL) and extracted with  $\text{CH}_2\text{Cl}_2$  (4  $\times$  50 mL). The combined organic phases were extracted with 1 N HCl (4  $\times$  50 mL). The combined aqueous phases were washed

with  $\text{CH}_2\text{Cl}_2$  (1  $\times$  20 mL), then made basic (pH > 10) with solid NaOH (~10 g, with cooling). The aqueous phase was extracted with  $\text{CH}_2\text{Cl}_2$  (4  $\times$  50 mL). The combined organic phases were dried ( $\text{K}_2\text{CO}_3$ ), filtered, and concentrated. The residue was purified by reverse-phase HPLC ( $\text{C}_{18}$ ,  $\text{MeCN}$ - $\text{H}_2\text{O}$ , 0.1% TFA). Fractions containing the product were concentrated under reduced pressure until all of the  $\text{MeCN}$  was removed, made basic with 1 N NaOH (pH > 11), and exhaustively extracted with  $\text{CH}_2\text{Cl}_2$ . The combined organic phases were dried ( $\text{Na}_2\text{SO}_4$ ), filtered, and concentrated to provide amine **5** (720 mg, 28%) as a colorless oil:  $^1\text{H}$  NMR (400 MHz,  $\text{CDCl}_3$ )  $\delta$  ppm 7.46–7.18 (m, 5H), 3.45 (q,  $J$  = 6.65 Hz, 1H), 3.16–2.98 (m, 1H), 2.65 (t,  $J$  = 8.91 Hz, 3H), 2.30 (ddd,  $J$  = 11.48, 9.04, 5.47 Hz, 1H), 2.18 (d,  $J$  = 2.48 Hz, 4H), 1.97–1.82 (m, 1H), 1.82–1.66 (m, 2H), 1.49–1.28 (m, 6H), 0.02–0.01 (m, 9H);  $^{13}\text{C}$  NMR (100 MHz,  $\text{CDCl}_3$ )  $\delta$  ppm 145.44, 128.12, 128.09, 127.15, 65.17, 58.90, 53.52, 42.37, 32.33, 31.16, 30.90, 29.56, 20.84; HRMS (FAB)  $m/z$  231.1858 (231.1861 calcd for  $\text{C}_{15}\text{H}_{23}\text{N}_2$  M + H). Data for **4**:  $^1\text{H}$  NMR (400 MHz,  $\text{CDCl}_3$ )  $\delta$  ppm 7.45–7.07 (m, 5H), 3.52 (q,  $J$  = 6.75 Hz, 1H), 3.34–3.19 (m, 1H), 2.76–2.52 (m, 3H), 2.11 (dt,  $J$  = 10.80, 5.63 Hz, 1H), 2.03–1.84 (m, 2H), 1.84–1.70 (m, 1H), 1.51–1.34 (m, 6H), 1.29 (m, 5H);  $^{13}\text{C}$  NMR (100 MHz,  $\text{CDCl}_3$ )  $\delta$  ppm 145.06, 128.10, 127.45, 126.67, 76.24, 64.27, 58.56, 53.31, 42.04, 32.55, 31.40, 29.62, 23.45.

**(3aS,6R,6aR)-6-Azido-1-((R)-1-phenylethyl)octahydrocyclopenta[b]pyrrole (6)** and **(3aR,6S,6aS)-6-Azido-1-((R)-1-phenylethyl)octahydrocyclopenta[b]pyrrole (7)**. To a solution of amine **2** (6.71 g, 31.2 mmol) in  $\text{CH}_2\text{Cl}_2$  (70 mL) was added  $\text{I}_2$  (8.70 g, 34.3 mmol) portionwise over 20 min with vigorous stirring. After 2 h, LCMS indicated complete conversion to iodide **3**. The mixture was concentrated under reduced pressure to afford a dark-brown foam.

The residue from above was dissolved in acetone (100 mL) and water (40 mL). Sodium azide (10.1 g, 156 mmol) was added and the mixture stirred at room temperature for 2 h. Aqueous 1 N NaOH (50 mL) was added and the acetone removed under reduced pressure. Water (100 mL) was added and extracted with  $\text{CH}_2\text{Cl}_2$  (1  $\times$  100 mL, 2  $\times$  50 mL). The combined organic phases were dried ( $\text{K}_2\text{CO}_3$ ), filtered, and concentrated. The residue was purified by chromatography on a 4 cm  $\times$  20 cm column of  $\text{SiO}_2$  with slow elution of 2–4% ether–hexanes modified with 2% triethylamine to afford 2.36 g (32%) of **6** and 1.97 g (27%) of **7** which was carried on directly. Diagnostic data for **7**:  $^1\text{H}$  NMR (400 MHz,  $\text{CDCl}_3$ )  $\delta$  7.36–7.25 (m, 5H), 3.53 (q,  $J$  = 6.7, 1H), 3.09 (d,  $J$  = 4.0, 1H), 3.04–2.96 (m, 1H), 2.92 (d,  $J$  = 8.5, 1H), 2.71–2.58 (m, 1H), 2.31 (ddd,  $J$  = 11.5, 8.9, 5.6, 1H), 1.98–1.89 (m, 1H), 1.85–1.65 (m, 2H), 1.56–1.47 (m, 1H), 1.44–1.39 (m, 4H), 1.38–1.24 (m, 1H);  $^{13}\text{C}$  NMR (100 MHz,  $\text{CDCl}_3$ )  $\delta$  144.83, 128.59, 128.13, 127.55, 74.28, 68.07, 52.76, 41.91, 31.61, 30.10, 29.19, 20.59. Diagnostic data for **6**:  $^1\text{H}$  NMR (400 MHz,  $\text{CDCl}_3$ )  $\delta$  7.34–7.20 (m, 5H), 3.86 (d,  $J$  = 4.8, 1H), 3.55 (q,  $J$  = 6.8, 2H), 2.94 (d,  $J$  = 8.5, 1H), 2.70–2.60 (m, 3H), 2.08 (ddd,  $J$  = 11.6, 9.0, 5.5, 1H), 2.00–1.94 (m, 2H), 1.85–1.74 (m, 3H), 1.57 (d,  $J$  = 3.1, 1H), 1.52–1.46 (m, 2H), 1.44 (d,  $J$  = 6.8, 3H), 1.34–1.21 (m, 2H).

**Hydrogenation of 7 to 5**. A mixture of azide **7** (446 mg, 1.74 mmol), ethyl acetate (20 mL), and 10% Pd·C (200 mg) in a 100 mL round-bottom flask was evacuated and refilled 3 $\times$  with  $\text{H}_2$  and then maintained under  $\text{H}_2$  (1 atm) with vigorous stirring for 4 h. The mixture was filtered through Celite and concentrated to afford 377 mg (94%) of amine **5** as a colorless oil. Spectral data were identical to material prepared by aminolysis of iodide **3**.

**[(3aR,6S,6aS)-1-((R)-1-Phenylethyl)octahydrocyclopenta[b]pyrrol-6-yl]carbamic Acid 2-Trimethylsilylanyl ethyl Ester (8)**. To a mixture of amine **5** (377 mg, 1.64 mmol),  $\text{CH}_2\text{Cl}_2$  (6 mL), and saturated aqueous  $\text{NaHCO}_3$  (6 mL) was added 4-nitrophenyl 2-(trimethylsilyl)ethyl carbamate (510 mg, 1.80 mmol), and the mixture was stirred vigorously at room temperature for 14 h. The mixture was partitioned between 1 N NaOH (50 mL) and  $\text{CH}_2\text{Cl}_2$  (50 mL). The phases were separated, and the organic phase was washed with 1 N NaOH (3  $\times$  20 mL). The combined aqueous phases were extracted with  $\text{CH}_2\text{Cl}_2$  (1  $\times$  20 mL). The combined organic phases were dried ( $\text{K}_2\text{CO}_3$ ), filtered, and concentrated. The

residue was purified by flash chromatography (40 g of  $\text{SiO}_2$ , 0–10% ethyl acetate in hexanes with 2% triethylamine) to afford 397 mg (65%) of **8** as a colorless oil:  $^1\text{H}$  NMR (400 MHz,  $\text{CDCl}_3$ )  $\delta$  ppm 7.46–7.00 (m, 5H), 4.42–4.18 (m, 1H), 4.18–3.97 (m, 2H), 3.97–3.80 (m, 1H), 3.77–3.43 (m, 1H), 3.10–2.82 (m, 1H), 2.72–2.62 (m, 1H), 2.56 (d,  $J$  = 8.38 Hz, 1H), 2.36 (q,  $J$  = 9.29 Hz, 1H), 2.01–1.88 (m, 1H), 1.84–1.79 (m, 1H), 1.76–1.61 (m, 1H), 1.42–1.39 (m, 1H), 1.37 (d,  $J$  = 6.71 Hz, 3H), 1.28 (s, 1H), 0.92 (dd,  $J$  = 9.57, 7.59 Hz, 2H), 0.02–0.01 (m, 9H);  $^{13}\text{C}$  NMR (100 MHz,  $\text{CDCl}_3$ )  $\delta$  ppm 144.70, 128.00, 127.60, 126.60, 59.20, 49.15, 41.21, 31.48, 30.47, 30.21, 30.18, 17.71, –1.51; HRMS (FAB)  $m/z$  375.2474 (375.2468 calcd for  $\text{C}_{21}\text{H}_{35}\text{N}_2\text{O}_2\text{Si}$  M + H).

**(3aR,6S,6aS)-(Octahydrocyclopenta[b]pyrrol-6-yl)carbamic Acid 2-Trimethylsilylanyl ethyl Ester (9)**. A mixture of **8** (397 mg, 1.06 mmol), 20% Pd(OH) $_2$ ·C (120 mg), acetic acid (0.30 mL), and MeOH (15 mL) was evacuated and refilled with  $\text{H}_2$  3 $\times$  and then stirred vigorously under 1 atm of  $\text{H}_2$  for 2 h. The mixture was filtered through Celite, then concentrated. The residue was dissolved in  $\text{CH}_2\text{Cl}_2$  (50 mL) and washed with 1 N NaOH (3  $\times$  20 mL). The combined aqueous phases were extracted with  $\text{CH}_2\text{Cl}_2$  (1  $\times$  20 mL). The combined organic phases were dried ( $\text{K}_2\text{CO}_3$ ), filtered, and concentrated to afford 265 mg (92%) of amine **9** as a colorless oil:  $^1\text{H}$  NMR (400 MHz,  $\text{CDCl}_3$ )  $\delta$  ppm 4.81–4.56 (m, 1H), 4.10 (m, 2H), 3.69–3.50 (m, 1H), 3.46–3.28 (m, 1H), 2.85 (t,  $J$  = 6.28 Hz, 2H), 2.67–2.50 (m, 1H), 2.28 (s, 1H), 1.96 (dt,  $J$  = 11.67, 5.67 Hz, 1H), 1.91–1.69 (m, 2H), 1.50–1.16 (m, 4H), 1.09–0.85 (m, 2H), 0.02–0.01 (m, 9H);  $^{13}\text{C}$  NMR (100 MHz,  $\text{CDCl}_3$ )  $\delta$  ppm 69.82, 62.82, 46.14, 40.87, 33.44, 31.48, 31.46, 30.35, 17.73, –1.53; HRMS (FAB)  $m/z$  271.1836 (271.1842 calcd for  $\text{C}_{13}\text{H}_{27}\text{N}_2\text{O}_2\text{Si}$  M + H).

**[(3aR,6S,6aS)-1-((S)-2-Benzoyloxycarbonylamino-3,3-dimethylbutyryl)octahydrocyclopenta[b]pyrrol-6-yl]carbamic Acid 2-Trimethylsilylanyl ethyl Ester (10)**. A mixture of amine **9** (437 mg, 1.62 mmol), Cbz-*N*-*tert*-butylglycine (514 mg, 1.94 mmol), HATU (1.23 g, 3.23 mmol), DIPEA (1.4 mL, 8.1 mmol), and DMF (10 mL) was maintained at room temperature 4 h. The mixture was diluted with ethyl acetate (100 mL) and washed with 1 N HCl (3  $\times$  20 mL). The combined aqueous phases were extracted with ethyl acetate (1  $\times$  10 mL). The combined organic phases were dried ( $\text{Na}_2\text{SO}_4$ ), filtered, and concentrated. The residue was purified by flash chromatography (40 g column  $\text{SiO}_2$ , 0–40% ethyl acetate–hexanes) to afford 485 mg (58%) of the product as a colorless oil, which was carried on directly. HRMS (FAB)  $m/z$  569.3741 (569.3734 calcd for  $\text{C}_{28}\text{H}_{53}\text{N}_4\text{O}_6\text{Si}$  M + H).

**[(3aR,6S,6aS)-1-((S)-2-Amino-3,3-dimethylbutyryl)octahydrocyclopenta[b]pyrrol-6-yl]carbamic Acid 2-Trimethylsilylanyl ethyl Ester (11)**. A mixture of the amide **10** (500 mg, 0.97 mmol), MeOH (20 mL), AcOH (0.8 mL), and 20% Pd(OH) $_2$ ·C (200 mg) was stirred vigorously under 1 atm of  $\text{H}_2$  for 3 h. The mixture was filtered through Celite with MeOH. The MeOH was removed under reduced pressure, and the residue was dissolved in  $\text{CH}_2\text{Cl}_2$  (50 mL) and washed with 0.5 N NaOH (3  $\times$  10 mL), dried ( $\text{Na}_2\text{SO}_4$ ), filtered, and concentrated to afford 300 mg (81%) of amine **11** as a colorless oil:  $^1\text{H}$  NMR (400 MHz,  $\text{CDCl}_3$ )  $\delta$  ppm 6.31–5.85 (m, 1H), 4.31 (dd,  $J$  = 8.79, 6.99 Hz, 1H), 4.20–4.00 (m, 2H), 3.72–3.62 (m, 1H), 3.57–3.44 (m, 2H), 3.26 (s, 1H), 2.67 (d,  $J$  = 6.66 Hz, 1H), 2.41–2.24 (m, 1H), 2.01 (m, 2H), 1.43–1.30 (m, 1H), 1.06–0.86 (m, 11H), 1.75–1.44 (m, 5H), 0.02–0.01 (m, 9H);  $^{13}\text{C}$  NMR (100 MHz,  $\text{CDCl}_3$ )  $\delta$  ppm 173.89, 157.07, 156.11, 67.31, 62.60, 60.07, 59.80, 47.69, 39.30, 35.49, 33.26, 31.76, 28.95, 26.20, 17.61, –1.50, –1.53; HRMS (FAB)  $m/z$  384.2690 (384.2682 calcd for  $\text{C}_{19}\text{H}_{38}\text{N}_3\text{O}_3\text{Si}$  M + H).

**(3aR,6S,6aS)-1-((S)-2-((S)-2-(*tert*-Butoxycarbonylmethylamino)propionylamino)-3,3-dimethylbutyryl)octahydrocyclopenta[b]pyrrol-6-yl]carbamic Acid 2-Trimethylsilylanyl ethyl Ester (12)**. To a solution of amine **11** (300 mg, 0.79 mmol) in acetonitrile (3.0 mL) were added *N*-Boc-*N*-methylalanine (185 mg, 0.090 mmol), DMAP (catalytic), and EDC (172 mg, 0.09 mmol), and the solution was stirred at room temperature for 1.5 h. The solution was diluted with  $\text{CH}_2\text{Cl}_2$  (50 mL) and then washed with 1 N HCl (3  $\times$  10 mL), 1 N NaOH (3  $\times$  10 mL), brine (1  $\times$  10 mL), dried

(Na<sub>2</sub>SO<sub>4</sub>), filtered, and concentrated to afford 426 mg (93%) of **12** as a colorless oil, which was used without further purification: <sup>1</sup>H NMR (400 MHz, CDCl<sub>3</sub>) δ ppm 7.40–7.26 (m, 5H), 5.85–5.67 (m, 1H), 5.61–5.55 (m, 1H), 5.20–5.00 (m, 3H), 4.35–4.21 (m, 2H), 4.20–4.05 (m, 3H), 3.90–3.80 (m, 1H), 3.60–3.45 (m, 2H), 2.35–2.20 (m, 1H), 2.05–1.85 (m, 3H), 1.85–1.45 (m, 3H), 1.45–1.35 (m, 1H), 1.10–0.90 (m, 11H), 0.10–0.90 (m, 9H); <sup>13</sup>C NMR (100 MHz, CDCl<sub>3</sub>) δ ppm 171.11, 170.33, 156.85, 156.14, 67.26, 62.59, 59.65, 56.33, 47.88, 39.38, 35.78, 35.52, 33.22, 31.62, 29.81, 29.63, 28.92, 28.29, 26.32, 17.56, –1.54; HRMS (FAB) *m/z* 569.3741 (569.3734 calcd for C<sub>28</sub>H<sub>53</sub>N<sub>4</sub>O<sub>6</sub>Si M + H).

**{(S)-1-[(S)-1-((3aR,6S,6aS)-6-Aminohexahydrocyclopenta[b]pyrrole-1-carbonyl)-2,2-dimethylpropylcarbamoyl]ethyl}methylcarbamoyl tert-Butyl Ester (13)**. Protected amine **12** (420 mg) was treated with excess TAS-F in MeCN (10 mL) at 50 °C for 18 h. The mixture was diluted with CH<sub>2</sub>Cl<sub>2</sub> (50 mL) and washed with 0.5 N NaOH (3 × 30 mL), dried (Na<sub>2</sub>SO<sub>4</sub>), filtered, and concentrated to afford quantitative yield of amine **13** as a colorless oil: <sup>1</sup>H NMR (400 MHz, CDCl<sub>3</sub>) δ ppm 6.94–6.49 (m, 1H), 4.80–4.48 (m, 2H), 3.98–3.92 (m, 1H), 3.91–3.80 (m, 1H), 3.48–3.35 (m, 1H), 3.26–3.14 (m, 1H), 3.05–2.98 (m, 1H), 2.76 (s, 5H), 2.04–1.77 (m, 3H), 1.77–1.52 (m, 3H), 1.52–1.40 (m, 11H), 1.40–1.19 (m, 6H), 1.01–0.79 (m, 10H); <sup>13</sup>C NMR (100 MHz, CDCl<sub>3</sub>) δ ppm 171.02, 170.94, 169.73, 169.71, 71.96, 60.62, 60.60, 56.51, 47.16, 41.30, 35.74, 34.77, 30.19, 29.82, 28.29, 26.41; HRMS (FAB) *m/z* 425.3130 (425.3128 calcd for C<sub>22</sub>H<sub>41</sub>N<sub>4</sub>O<sub>4</sub> M + H).

**Naphthalene-1-carboxylic Acid {(3aR,6S,6aS)-1-[(S)-3,3-Dimethyl-2-((S)-2-methylaminopropionylamino)butyryl]octahydrocyclopenta[b]pyrrol-6-yl}amide (14b)**. To a solution of amine **13** (84 mg, 0.20 mmol) and MeCN (1 mL) were added 1-naphthoic acid (42 mg, 0.24 mmol), DMAP (catalytic), and EDC (46 mg, 0.24 mmol), and the mixture was stirred at room temperature for 1 h. The mixture was diluted with CH<sub>2</sub>Cl<sub>2</sub> (50 mL), washed with 1 N HCl (1 × 50 mL), 1 N NaOH (1 × 50 mL), brine (1 × 50 mL), dried (Na<sub>2</sub>SO<sub>4</sub>), filtered, and concentrated. The residue was chromatographed (SiO<sub>2</sub>, 60% ethyl acetate–hexanes) to afford 84 mg of the *N*-Boc-protected intermediate.

The residue from above was dissolved in CH<sub>2</sub>Cl<sub>2</sub> (2 mL) and TFA (1 mL) and maintained at room temperature for 2 h. The solvents were removed under reduced pressure, and the residue was purified by HPLC, and the solvents were removed by lyophilization to afford 43 mg (28%) of **14b** as a colorless powder: *t<sub>R</sub>* (C18) = 3.98 min; *t<sub>R</sub>* (SFCd) = 3.47 min; MS *m/z* = 479 (M + H<sup>+</sup>).

**Benzeneacetamide, N-[(3aR,6S,6aS)-Octahydro-1-(*N*-methyl-L-alanyl-3-methyl-L-valyl)cyclopenta[b]pyrrol-6-yl]-α-phenyl- (14a)**. Yield, 71%; *t<sub>R</sub>* (C18) = 4.59 min; *t<sub>R</sub>* (SFCd) = 3.18 min; MS *m/z* = 519 (M + H<sup>+</sup>).

**4-Fluoronaphthalene-1-carboxylic Acid {(3aR,6S,6aS)-1-[(S)-3,3-Dimethyl-2-((S)-2-methylaminopropionylamino)butyryl]octahydrocyclopenta[b]pyrrol-6-yl}amide (14c)**. Yield, 33%; *t<sub>R</sub>* (C18) = 4.30 min; *t<sub>R</sub>* (SFCd) = 3.29 min; MS *m/z* = 497 (M + H<sup>+</sup>).

**4-Methylnaphthalene-1-carboxylic Acid {(3aR,6S,6aS)-1-[(S)-3,3-Dimethyl-2-((S)-2-methylaminopropionylamino)butyryl]octahydrocyclopenta[b]pyrrol-6-yl}amide (14d)**. Yield, 39%; *t<sub>R</sub>* (C18) = 4.16 min; *t<sub>R</sub>* (SFCd) = 3.44 min; MS *m/z* = 493 (M + H<sup>+</sup>).

**2-Methoxy-naphthalene-1-carboxylic Acid {(3aR,6S,6aS)-1-[(S)-3,3-Dimethyl-2-((S)-2-methylaminopropionylamino)butyryl]octahydrocyclopenta[b]pyrrol-6-yl}amide (14e)**. Yield, 52%; *t<sub>R</sub>* (C18) = 3.98 min; *t<sub>R</sub>* (SFCd) = 3.56 min; MS *m/z* = 509 (M + H<sup>+</sup>).

**Naphthalene-2-carboxylic Acid {(3aR,6S,6aS)-1-[(S)-3,3-Dimethyl-2-((S)-2-methylaminopropionylamino)butyryl]octahydrocyclopenta[b]pyrrol-6-yl}amide (14f)**. Yield, 79%; *t<sub>R</sub>* (C18) = 4.24 min; *t<sub>R</sub>* (SFCd) = 3.41 min; MS *m/z* = 479 (M + H<sup>+</sup>).

**Cell Viability Assays.** Cells were dissociated from tissue culture flasks by incubation with Accutase (Innovative Cell Technology

Inc.; San Diego, CA) for 5–10 min. The detached cells were washed with phosphate buffered saline (PBS) and resuspended in assay media. Cells were placed in tissue culture-treated, white-wall, clear-bottom, 96-well plates (Corning, Inc.; Corning, NY) at 1 × 10<sup>4</sup> cells/well in a volume of 50 μL. The plates were incubated at 37 °C in 5% CO<sub>2</sub> overnight.

The next day, the media were removed and compounds added to the cells in assay media. Plates were incubated at 37 °C in 5% CO<sub>2</sub> for 3–4 days before cell viability was measured using the CellTiter-Glo luminescent cell viability assay kit (Promega Corp.; Madison, WI) according to the manufacturer's instructions.

**Caspase-3/7 Assays.** Cells seeded in black-wall, clear-bottom plates were incubated at 37 °C and 5% CO<sub>2</sub> for 3–24 h before caspase-3 and -7 activities were assessed using the Apo-ONE homogeneous caspase-3/7 assay kit (Promega Corp.; Madison, WI) according to the manufacturer's instructions.

**Western Blot Analysis.** Western blot analysis was performed as described previously<sup>25,26</sup> using the following lysis buffer: 1% Triton X-100, 150 mM NaCl, 50 mM Tris, pH 7.5, 5 mM EDTA, protease inhibitory cocktail (Roche). The primary antibodies against c-IAP1 were purchased from R&D (affinity-purified goat antibody) and against Beta Tubulin from MP Biopharmaceuticals (mouse monoclonal).

**Inhibition of MDA-MB-231-X1.1 Xenograft Tumor Growth by IAP Antagonists.** All procedures involving animals were performed in accordance with Genentech's Institutional Animal Care and Use Committee guidelines. To generate tumors, 100 μL of a single-cell suspension containing 1 × 10<sup>7</sup> MDA-MB-231-X1.1 cells (in-house GFP-expressing variants of MDA-MB-231 cells (ATCC, Manassas, VA)) were injected subcutaneously into the upper right flanks of 8-week-old female C.B-17 SCID.bg mice (Charles River Laboratories, Hollister, CA). Tumor volume was calculated using the mean diameter measured with vernier calipers using the formula  $v = 0.5ab^2$ , where *a* and *b* are the smallest and largest perpendicular tumor diameters, respectively. Once-daily administration of IAP antagonists by oral gavage was initiated once tumors reached a size of ~200 mm<sup>3</sup> (~1.5 weeks after inoculation). IAP antagonists were formulated in 15% hydroxypropyl-β-cyclodextrin and 20 mM succinic acid and administered in a volume of 100 μL. Tumor volumes and body weights were measured twice weekly until end of study.

**Acknowledgment.** We thank members of the DMPK and Purification groups within Genentech Small Molecule Drug Discovery for analytical support. X-ray crystallographic data were collected at The Advanced Light Source and Berkeley Center for Structural Biology which are supported in part by the U.S. Department of Energy and the National Institutes of Health.

**Supporting Information Available:** Experimental procedures for synthesis and characterization of additional IAP antagonists, table of additional antagonists and potency in FP assay, and X-ray data collection and refinement statistics. This material is available free of charge via the Internet at <http://pubs.acs.org>.

## References

- Salvesen, G. S.; Duckett, C. S. IAP proteins: blocking the road to death's door. *Nat. Rev. Mol. Cell Biol.* **2002**, *3*, 401–410.
- Varfolomeev, E.; Blankenship, J. W.; Wayson, S. M.; Fedorova, A. V.; Kayagaki, N.; Garg, P.; Zobel, K.; Dynek, J. N.; Elliott, L. O.; Wallweber, H. J.; Flygare, J. A.; Fairbrother, W. J.; Deshayes, K.; Dixit, V. M.; Uvic, D. IAP antagonists induce autoubiquitination of c-IAPs, NF-κB activation, and TNFα-dependent apoptosis. *Cell* **2007**, *131*, 669–681.
- Varfolomeev, E.; Goncharov, T.; Fedorova, A. V.; Dynek, J. N.; Zobel, K.; Deshayes, K.; Fairbrother, W. J.; Uvic, D. c-IAP1 and c-IAP2 are critical mediators of TNFα-induced NF-κB activation. *J. Biol. Chem.* **2008**, *283*, 24295–24299.
- Vince, J. E.; Wong, W. W.; Khan, N.; Feltham, R.; Chau, D.; Ahmed, A. U.; Benetatos, C. A.; Chunduru, S. K.; Condon, S. M.; McKinlay,

- M.; Brink, R.; Leverkus, M.; Tergaonkar, V.; Schneider, P.; Callus, B. A.; Koentgen, F.; Vaux, D. L.; Silke, J. IAP antagonists target cIAP1 to induce TNF $\alpha$ -dependent apoptosis. *Cell* **2007**, *131*, 682–693.
- (5) Bertrand, M. J.; Milutinovic, S.; Dickson, K. M.; Ho, W. C.; Boudreault, A.; Durkin, J.; Gillard, J. W.; Jaquith, J. B.; Morris, S. J.; Barker, P. A. cIAP1 and cIAP2 facilitate cancer cell survival by functioning as E3 ligases that promote RIP1 ubiquitination. *Mol. Cell* **2008**, *30*, 689–700.
- (6) Mahoney, D. J.; Cheung, H. H.; Mrad, R. L.; Plenchette, S.; Simard, C.; Enwere, E.; Arora, V.; Mak, T. W.; Lacasse, E. C.; Waring, J.; Korneluk, R. G. Both cIAP1 and cIAP2 regulate TNF $\alpha$ -mediated NF- $\kappa$ B activation. *Proc. Natl. Acad. Sci. U.S.A.* **2008**, *105*, 11778–11783.
- (7) Fesik, S. W. Promoting apoptosis as a strategy for cancer drug discovery. *Nat. Rev. Cancer* **2005**, *5*, 876–885.
- (8) Vucic, D.; Fairbrother, W. J. The inhibitor of apoptosis proteins as therapeutic targets in cancer. *Clin. Cancer Res.* **2007**, *13*, 5995–6000.
- (9) Sun, H.; Nikolovska-Coleska, Z.; Yang, C. Y.; Xu, L.; Liu, M.; Tomita, Y.; Pan, H.; Yoshioka, Y.; Krajewski, K.; Roller, P. P.; Wang, S. Structure-based design of potent, conformationally constrained Smac mimetics. *J. Am. Chem. Soc.* **2004**, *126*, 16686–16687.
- (10) Zobel, K.; Wang, L.; Varfolomeev, E.; Franklin, M. C.; Elliott, L. O.; Wallweber, H. J.; Okawa, D. C.; Flygare, J. A.; Vucic, D.; Fairbrother, W. J.; Deshayes, K. Design, synthesis, and biological activity of a potent Smac mimetic that sensitizes cancer cells to apoptosis by antagonizing IAPs. *ACS Chem. Biol.* **2006**, *1*, 525–533.
- (11) Li, L.; Thomas, R. M.; Suzuki, H.; De Brabander, J. K.; Wang, X.; Harran, P. G. A small molecule Smac mimic potentiates TRAIL- and TNF $\alpha$ -mediated cell death. *Science* **2004**, *305*, 1471–1474.
- (12) Park, C. M.; Sun, C.; Olejniczak, E. T.; Wilson, A. E.; Meadows, R. P.; Betz, S. F.; Elmore, S. W.; Fesik, S. W. Non-peptidic small molecule inhibitors of XIAP. *Bioorg. Med. Chem. Lett.* **2005**, *15*, 771–775.
- (13) Wu, T. Y.; Wagner, K. W.; Bursulaya, B.; Schultz, P. G.; Deveraux, Q. L. Development and characterization of nonpeptidic small molecule inhibitors of the XIAP/caspase-3 interaction. *Chem. Biol.* **2003**, *10*, 759–767.
- (14) Schimmer, A. D.; Welsh, K.; Pinilla, C.; Wang, Z.; Krajewska, M.; Bonneau, M. J.; Pedersen, I. M.; Kitada, S.; Scott, F. L.; Bailly-Maitre, B.; Glinsky, G.; Scudiero, D.; Sausville, E.; Salvesen, G.; Nefzi, A.; Ostresh, J. M.; Houghten, R. A.; Reed, J. C. Small-molecule antagonists of apoptosis suppressor XIAP exhibit broad antitumor activity. *Cancer Cell* **2004**, *5*, 25–35.
- (15) Nikolovska-Coleska, Z.; Xu, L.; Hu, Z.; Tomita, Y.; Li, P.; Roller, P. P.; Wang, R.; Fang, X.; Guo, R.; Zhang, M.; Lippman, M. E.; Yang, D.; Wang, S. Discovery of embelin as a cell-permeable, small-molecular weight inhibitor of XIAP through structure-based computational screening of a traditional herbal medicine three-dimensional structure database. *J. Med. Chem.* **2004**, *47*, 2430–2440.
- (16) Huang, J. W.; Zhang, Z.; Wu, B.; Cellitti, J. F.; Zhang, X.; Dahl, R.; Shiao, C. W.; Welsh, K.; Emdadi, A.; Stebbins, J. L.; Reed, J. C.; Pellecchia, M. Fragment-based design of small molecule X-linked inhibitor of apoptosis protein inhibitors. *J. Med. Chem.* **2008**, *51*, 7111–7118.
- (17) Oost, T. K.; Sun, C.; Armstrong, R. C.; Al-Assaad, A. S.; Betz, S. F.; Deckwerth, T. L.; Ding, H.; Elmore, S. W.; Meadows, R. P.; Olejniczak, E. T.; Oleksijew, A.; Oltersdorf, T.; Rosenberg, S. H.; Shoemaker, A. R.; Tomaselli, K. J.; Zou, H.; Fesik, S. W. Discovery of potent antagonists of the antiapoptotic protein XIAP for the treatment of cancer. *J. Med. Chem.* **2004**, *47*, 4417–4426.
- (18) Chauhan, D.; Neri, P.; Velankar, M.; Podar, K.; Hideshima, T.; Fulciniti, M.; Tassone, P.; Raje, N.; Mitsiades, C.; Mitsiades, N.; Richardson, P.; Zavel, L.; Tran, M.; Munshi, N.; Anderson, K. C. Targeting mitochondrial factor Smac/DIABLO as therapy for multiple myeloma (MM). *Blood* **2007**, *109*, 1220–1227.
- (19) Lauri, G.; Bartlett, P. A. CAVEAT: a program to facilitate the design of organic molecules. *J. Comput.-Aided Mol. Des.* **1994**, *8*, 51–66.
- (20) Vucic, D.; Franklin, M. C.; Wallweber, H. J.; Das, K.; Eckelman, B. P.; Shin, H.; Elliott, L. O.; Kadhodayan, S.; Deshayes, K.; Salvesen, G. S.; Fairbrother, W. J. Engineering ML-IAP to produce an extraordinarily potent caspase 9 inhibitor: implications for Smac-dependent anti-apoptotic activity of ML-IAP. *Biochem. J.* **2005**, *385*, 11–20.
- (21) Friesner, R. A.; Banks, J. L.; Murphy, R. B.; Halgren, T. A.; Klicic, J. J.; Mainz, D. T.; Repasky, M. P.; Knoll, E. H.; Shelley, M.; Perry, J. K.; Shaw, D. E.; Francis, P.; Shenkin, P. S. Glide: a new approach for rapid, accurate docking and scoring. 1. Method and assessment of docking accuracy. *J. Med. Chem.* **2004**, *47*, 1739–1749.
- (22) Corey, E. J.; Chen, C.-P.; Reichard, G. A. (+)-1(S),5(R),8(S)-8-Phenyl-2-azabicyclo[3.3.0]octane-8-ol *N,O*-methylboronate and its enantiomer, chiral chemzymes which serve as catalysts for their own enantioselective synthesis. *Tetrahedron Lett.* **1989**, *30*, 5547–5550.
- (23) Kawabata, T.; Nagato, M.; Takasu, K.; Fujii, K. Nonenzymatic kinetic resolution of racemic alcohols through an “induced fit” process. *J. Am. Chem. Soc.* **1997**, *119*, 3169–3170.
- (24) Scheidt, K. A.; Chen, H.; Follows, B. C.; Chemler, S. R.; Coffey, D. S.; Roush, W. R. Tris(dimethylamino)sulfonium difluorotrimethylsilicate, a mild reagent for the removal of silicon protecting groups. *J. Org. Chem.* **1998**, *63*, 6436–6437.
- (25) Varfolomeev, E.; Wayson, S. M.; Dixit, V. M.; Fairbrother, W. J.; Vucic, D. The inhibitor of apoptosis protein fusion c-IAP2.MALT1 stimulates NF- $\kappa$ B activation independently of TRAF1 AND TRAF2. *J. Biol. Chem.* **2006**, *281*, 29022–29029.
- (26) Vucic, D.; Stennicke, H. R.; Pisabarro, M. T.; Salvesen, G. S.; Dixit, V. M. ML-IAP, a novel inhibitor of apoptosis that is preferentially expressed in human melanomas. *Curr. Biol.* **2000**, *10*, 1359–1366.

JM801450C